

# Microstructure and compressive properties of multicomponent $\text{Al}_x(\text{TiVCrMnFeCoNiCu})_{100-x}$ high-entropy alloys

Y.J. Zhou\*, Y. Zhang, Y.L. Wang, G.L. Chen

State Key Laboratory for Advanced Metals and Materials, University of Science and Technology Beijing, Beijing 100083, China

Received 2 October 2006; received in revised form 3 November 2006; accepted 7 November 2006

## Abstract

The microstructure and compressive properties of  $\text{Al}_x(\text{TiVCrMnFeCoNiCu})_{100-x}$  ( $x = 0, 11.1, 20$  and  $40$  at.%) high-entropy alloys were studied. With the increase of Al content, the number of phases in the alloys gradually decreases. When Al content is  $20$  at.%, only bcc solid-solution structure is found in the alloy. The effect of high mixing entropy does facilitate the formation of simple solid solutions, making the total number of phases well below the maximum equilibrium number allowed by the Gibbs phase rule. The solid-solution strengthening mechanism and the structure transformation from fcc to bcc make the alloys have fairly high compressive strength; among them the compressive strength of  $\text{Al}_{11.1}(\text{TiVCrMnFeCoNiCu})_{88.9}$  alloy reaches  $2.431$  GPa.

© 2006 Elsevier B.V. All rights reserved.

**Keywords:** High-entropy alloy; Microstructure; Compressive properties

## 1. Introduction

Conventional strategy for developing new alloys is based on one or two elements as major constituent, and other minor elements as their constituents for the enhancement of definite properties. The main reason for not incorporating multi-principal elements into alloy preparation is the anticipated formation of many intermetallic compounds and complex microstructures, which would make alloys brittle and difficult in processing and analysis [1].

Recently, a new alloy system called “high-entropy alloy” (i.e. HEA) was developed and the cognitive strategy of alloy design was broken through [2,3]. HEA contains multi-elements as its major constituents, and each constituent element in the system could be regarded as a solute atom. To increase the entropy, each major element of the alloy system is in equimolar or near-equimolar ratio.

The microstructure and compressive properties of  $\text{Al}_x(\text{TiVCrMnFeCoNiCu})_{100-x}$  ( $x = 0, 11.1, 20$  and  $40$  at.%) high-entropy alloys were studied in this paper. Our purpose is, by the research of the new alloys, to investigate its properties and potential applications.

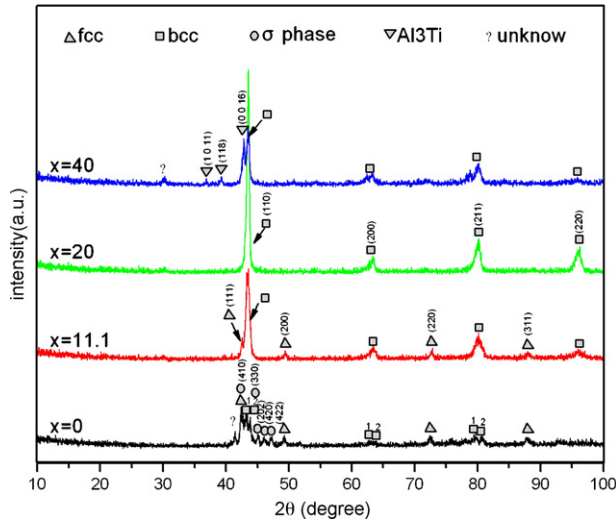
## 2. Experimental

HEA (i.e.  $\text{Ti}_{12.5}\text{V}_{12.5}\text{Cr}_{12.5}\text{Mn}_{12.5}\text{Fe}_{12.5}\text{Co}_{12.5}\text{Ni}_{12.5}\text{Cu}_{12.5}$ ) was prepared as intermediate alloy from commercial-purity elements (purity better than  $99$  wt.%) by medium-frequency induction melting under inert atmosphere. This alloy was then melted with Al ( $99.7$  wt.%) to obtain alloy ingots with nominal composition of  $\text{Al}_x(\text{HEA})_{100-x}$  ( $x = 0, 11.1, 20$  and  $40$  at.%) alloys by arc melting in a Ti-gettered argon atmosphere. The alloys were remelted four times to improve homogeneity. After that, the ingots were inductively melted in quartz tube under a vacuum ( $10^{-3}$  Pa), and then injection cast into a water-cooled copper mould with diameter of  $5$  mm and length of  $70$  mm.

The structure of the cylindrical alloys (cross-sectional surface) was characterized by X-ray diffraction (XRD) using a MXP21VAHF diffractometer with Cu  $K\alpha$  radiation. The morphology and composition of as-cast specimens were examined with a LEO-1450 scanning electron microscope (SEM) with energy dispersive spectrometry (EDS). Thin-foil specimens were prepared by mechanical thinning followed by ion milling, and subsequently observed using a JEM-2000 high resolution transmission electron microscope (HRTEM). For compressive tests, samples with  $5$  mm in diameter and  $10$  mm in height were prepared and investigated with MTS 809 materials testing machine at room temperature with a strain rate of  $1 \times 10^{-4} \text{ s}^{-1}$ . A Cambridge S250MK2 scanning electron microscope was

\* Corresponding author. Tel.: +86 10 62322160; fax: +86 10 62332508.

E-mail addresses: jxgznd.zyj@yahoo.com.cn, jxgznd.zyj@163.com (Y.J. Zhou), drzhangy@skl.ustb.edu.cn (Y. Zhang).

Fig. 1. XRD patterns of  $\text{Al}_x(\text{HEA})_{100-x}$  alloys.

used to study the fracture surface of the compression test samples.

### 3. Results

#### 3.1. Structural characterization

The XRD patterns of the as-cast alloys are presented in Fig. 1. The structure of  $\text{Al}_0\text{HEA}_{100}$  alloy is rather complex. Both fcc and bcc solid-solution structures, together with  $\sigma$  phase and a few unknown phases are found in this alloy. The broad diffraction peak at  $2\theta = 42\text{--}47^\circ$  in its pattern indicates that amorphous phase exists in  $\text{Al}_0\text{HEA}_{100}$  alloy. With the increase of Al content, the number of phases gradually decreases. For  $\text{Al}_{11.1}\text{HEA}_{88.9}$  alloy, except for fcc and bcc reflections, no other phases can be found. From the strongest XRD peak, the lattice parameters of fcc and bcc are estimated to be 0.3673 and 0.2934 nm, respectively. When Al content reaches 20 at.%, only bcc solid-solution structure can be found in the alloy. As Al content increases to 40 at.%, intermetallic phases, such as  $\text{Al}_3\text{Ti}$  and some other unknown ordered phases, present besides bcc solid solution. Thus, the addition of Al makes the alloys gradually transform from fcc into stabilized bcc, but too much Al leads to the precipitation of brittle intermetallic phases such as  $\text{Al}_3\text{Ti}$ .

Fig. 2 shows the SEM backscattered electron images of the alloys. The chemical compositions derived from EDS analysis are listed in Table 1. All the alloys exhibit a typical cast dendrite structure, with the dendrite size and morphology similar to each other. The dendrites are round and irregular with an average primary arm width of 8–14  $\mu\text{m}$ . As shown in Fig. 2(a), the dendrites of  $\text{Al}_0\text{HEA}_{100}$  alloy contain multiphases. For  $\text{Al}_{11.1}\text{HEA}_{88.9}$  alloy, dendrites consist of bcc single phase, while interdendrites exhibit eutectic structure obviously (as shown in Fig. 2(b)), that is, fcc and bcc coexist. For  $\text{Al}_{20}\text{HEA}_{80}$  alloy, both the dendrites and interdendrites are composed of bcc single phase as shown in Fig. 2(c). For the three alloys above, Cu segregates preferentially to the interdendrites, it is reasonable to deduce that the interdendrites are mainly composed of solid solution in which Cu is solvent. The serious Cu segregation should be attributed to the small bonding energies of Cu with other atoms for which Cu is rejected into the interdendrite region. The interdendrites of  $\text{Al}_{40}\text{HEA}_{60}$  alloy show multiphases, both needle-like phase and some other order phases precipitated can be observed in Fig. 2(d). According to XRD and EDS analysis, these phases are identified to be  $\text{Al}_3\text{Ti}$  and an ordered intermetallic phase.

Fig. 3 shows the HRTEM and corresponding selected area inverse fast Fourier transform (IFFT) images of  $\text{Al}_0\text{HEA}_{100}$  alloy. The ordered nanophase (as shown in Fig. 3(b)), inset fast Fourier transform (FFT) image and disordered matrix (as shown in Fig. 3(c)), confirm the existence of nanoparticles and amorphous phase, respectively. It can be seen in Fig. 3(a) that the dispersing nanoparticles are embedded in the amorphous matrix.

#### 3.2. Compressive properties

Fig. 4 shows the true stress–strain curves of room temperature compressive test for the alloys. Both  $\text{Al}_{11.1}\text{HEA}_{88.9}$  and  $\text{Al}_{20}\text{HEA}_{80}$  alloys exhibit fairly high compressive strength, some plastic deformation and slight work hardening capacity. The compressive strength and plastic strain of  $\text{Al}_{11.1}\text{HEA}_{88.9}$  alloy are 2.431 GPa and 0.95%, respectively. As for  $\text{Al}_{20}\text{HEA}_{80}$  alloy, its compressive strength is 2.016 GPa, and plastic strain is 2.35%. Both  $\text{Al}_0\text{HEA}_{100}$  and  $\text{Al}_{40}\text{HEA}_{60}$  alloys exhibit brittle fracture, with compressive strengths of 1.312 and 1.461 GPa, respectively. The Young's modulus ( $E$ ), yield strength  $\sigma_y$ , com-

Table 1  
Chemical compositions of as-cast Al–HEA alloy system (at.%)

Alloy	Region	Al	Ti	V	Cr	Mn	Fe	Co	Ni	Cu
$\text{Al}_0\text{HEA}_{100}$	Dendrite	0	23.38	9.78	5.60	9.95	11.22	18.60	15.71	5.77
	Interdendrite	0	1.76	0.37	0.75	22.17	1.13	0.79	8.18	64.86
$\text{Al}_{11.1}\text{HEA}_{88.9}$	Dendrite	14.48	9.81	17.28	17.32	2.82	12.78	12.38	9.67	3.46
	Interdendrite	4.37	1.14	0.63	0.75	11.71	1.48	1.18	4.19	74.55
$\text{Al}_{20}\text{HEA}_{80}$	Dendrite	23.61	10.58	11.90	10.94	6.90	10.30	11.53	9.77	4.47
	Interdendrite	20.55	0.55	0.37	0.70	22.28	0.92	0.43	3.74	50.46
$\text{Al}_{40}\text{HEA}_{60}$	Dendrite	37.97	3.82	19.70	19.96	3.51	6.87	2.59	2.50	3.08
	Interdendrite	51.38	15.02	6.18	3.21	2.01	6.41	7.40	6.45	1.95

Download English Version:

<https://daneshyari.com/en/article/1584263>

Download Persian Version:

<https://daneshyari.com/article/1584263>

[Daneshyari.com](https://daneshyari.com)